IEEE Access
Multidisciplinary | Rapid Review | Open Access Journal

Received November 9, 2021, accepted November 16, 2021, date of publication November 18, 2021,
date of current version November 30, 2021.

Digital Object Identifier 10.1109/ACCESS.2021.3129263

Enhancing the Braking Performance of a Vehicle Through the Proper Control of the Active Suspension System

DIMITRIOS PAPAGIANNIS, EVANGELOS TSIOUMAS, MARKOS KOSEOGLOU, NIKOLAOS JABBOUR, AND CHRISTOS MADEMLIS, (Senior Member, IEEE)
School of Electrical and Computer Engineering, Aristotle University of Thessaloniki, 54124 Thessaloniki, Greece

Corresponding author: Dimitrios Papagiannis (dipapagi@auth.gr)

The research work was supported by the Hellenic Foundation for Research and Innovation (HFRI) under the HFRI PhD Fellowship grant (Fellowship Number: 117).

ABSTRACT This paper investigates the problem of the vehicle's braking performance and a control method is proposed that can reduce the stopping time and distance, through the proper control of the active suspension system. Specifically, a Linear Quadratic Controller is utilized, that regulates the vehicle's frame pitch angle during the braking process for establishing a correct balance between the front and rear axles. Moreover, a fuzzy-logic system is introduced, which penalizes the effort of the actuators aiming to the reduction of the consumed power. The proposed control method of the active suspension system is energized only in an emergency condition, which is identified through the travel of the braking pedal pushed by the driver. Under normal conditions, the active suspension returns to the regular operation, that is the improvement of the passengers' comfort by means of rejecting the vehicle's disturbances induced by road's irregularities. The effectiveness of the proposed emergency control technique of the active suspension system is verified through a simulation model, by using the MATLAB/Simulink software, in comparison to a passive, semi-active and an active suspension, as in the literature. Selective simulation results for various road conditions are presented to demonstrate the operating improvements.

INDEX TERMS Active suspension, braking system, vehicle control, active safety, emergency conditions.

I. INTRODUCTION

The vehicle suspension system refers to the group of mechanical components that connect the wheels to the body and plays a key role for both the passengers' comfort and the vehicle's handling response [1]. The suspension systems are mainly categorized in *passive*, *semi-active* and *active* depending on the construction and the control capabilities [2].

In a passive suspension, the rejection of the disturbances is accomplished by the cooperation of a spring and a damper, but without any control on their performance. The performance of the damper can be indirectly controlled in a semi-active suspension. However, full control can be attained in an active suspension and thus, increased capabilities for fast and fully controlled response are provided. Although the active suspensions are higher energy consumed and costly, compared to both passive and semi-active suspensions, their competitive advantages make them very attractive [2], if the improvement of the vehicle's behavior is desired [3].

An active suspension can effectively increase the passengers' comfort, compared to the passive and semi-active suspensions, by both isolating the vehicle's suspended mass from the road unevenness and absorbing its movement during the acceleration, deceleration, and cornering maneuvers [4]. Thus, a growing research interest has been observed in the last years and several research papers have been published in the technical literature on the fields of the control design and the implementation of the active suspension. Specifically, a theoretical study on the control problem of the active suspension by considering both ride and handling quality into the optimal control formulation has been presented in [5]. A practical implementation approach of the active suspension has been proposed in [6] and an active suspension system with tubular linear brushless permanent magnet motor drives has been

The associate editor coordinating the review of this manuscript and approving it for publication was Shihong Ding.

presented in [7]. The analytical design of a PID controller of an active vehicle suspension system, for enhancing the ride comfort, has been presented in [8]. Also, several research efforts to enhance the performance of the active suspension by utilizing the model predictive control technique have been reported in [9]–[11].

To compensate the influence of the uncertainties that the vehicle components may cause on the active suspension performance (e.g. the distribution of the vehicle's weight, actuator faults, etc.), several control methods have been proposed based on the robust control [12], [13], fault tolerance control [14], adaptive dynamic surface control [15], adaptive neural networks [16], [17], and fuzzy-logic control [18], [19]. The common goal of the aforementioned control methods is the reduction of the vertical acceleration of the sprung mass of the vehicle, by regulating the actuator force. However, since they are focused on the improvement of the passengers' comfort, they disregard the potential contribution of the active suspension on the vehicle's braking performance.

Since the active suspension can play a key role at the handling of the vehicle, several control techniques and implementation methods have been proposed. Specifically, the driving performance of a semi-active suspension based on a hybrid control strategy has been studied in [20]. A hybrid control system based on the skyhook and ground-hook methods has been proposed in [21], aiming to effectively reject the oscillations of the wheels in order to keep the contact with the road. The influence of the active suspension on the vehicle's yaw and lateral dynamics through the adjustment of the roll stiffness of the vehicle has been examined in [22], aiming to the proper control of the lateral load distribution between the front and rear axles, in order to increase the vehicle's stability during cornering maneuvers. An electric active stabilizer has been utilized in [23], in order to minimize the roll angle of the sprung mass and thus, to enhance the performance of the vehicle during cornering. Coordinated control strategies for active steering, active suspension and differential braking have been examined in [24] to improve the vehicle's stability during high-speed maneuvers. Also, the vehicle dynamics in quasi-state conditions with respect to the lateral dynamics have been examined in [25]. However, although the above publications thoroughly examine the lateral dynamic performance of the vehicle with an active suspension, they ignore the longitudinal dynamic response during the braking process.

It is well known that the braking performance of a vehicle is very important for the safety of the passengers and the pedestrians, as well as the safety with respect to the other vehicles. Thus, all modern cars are equipped with antilock braking systems (ABS), in order to enhance the effectiveness of the braking process [26]. The objective of the ABS is to ensure that the wheels of the vehicle will not be locked during a braking, and they can continue to roll to provide the required decelerating contact force [27]. This is realized by regulating the brake valve attaining the proper braking pressure with respect to the road's conditions. However, the ABS can only prevent the lock-up of the wheels, and thus, despite the proper regulation of the braking force to each wheel, loss of the vehicle's control may occur during the braking process [28]. To overcome this drawback, the electronic brakeforce distribution (EBD) has been developed that assists the ABS to distribute the correct braking force to each wheel according to the weight it supports. Specifically, the EBD measures the difference between the speed of the vehicle and the rotation of each tire and tries to keep it within acceptable limits by properly controlling the brake valve of each wheel [29], [30].

Although the combined systems of ABS and EBD can considerably improve the braking performance, they cannot effectively control the distribution of the vehicle's weight to the front and rear axles, since they have been designed for passive suspensions and thus, they act on the control of the pressure of the brake fluid [31]. Specifically, they cannot lift the front axle during the braking, in order to reduce its weight by transferring it to the rear axle and thus, to properly regulate the vertical tire forces so as, to increase the total braking force of the vehicle. Contrarily, a properly controlled active suspension system can improve the distribution of the vertical forces between the front and rear axles and hence, in conjunction with the ABS-EBD, it can considerably enhance the braking performance of the vehicle.

A control algorithm that can reduce the wheel load oscillations under ABS braking conditions for a vehicle running up to 70 km/h has been presented in [32]. A technique that reduces the braking distance of a vehicle through the proper control of a semi-active suspension system, by regulating the active damping between the two extrema, has been proposed in [33]. However, since the technique has been developed for semi-active suspensions, the reduction of the braking distance is confined to 1.3% for a smooth road and 3.5% for a very rough road, compared to a passive suspension system.

Although it is well known that an active suspension system can reinforce the response of the vehicle's braking during emergency conditions, only a few research efforts have been conducted to develop an effective control method. Specifically, a preliminary investigation towards the reduction of the braking distance through the proper control of the active suspension has been presented in [34], where the goal of the suspension system is to impose normal force synchronized with the brake torque. However, the effect of the normal force during the braking procedure has been examined individually for the front and rear tires and not for the whole vehicle and also, the potential loss of the tire's contact with the ground during the dynamic performance of the suspension has been disregarded. An ABS control method assisted by an active suspension system has been presented in [35]; however, the quarter car model has been considered and consequently, the longitudinal weight transfer has been ignored. From the above, it is revealed that a method that can properly control the vehicle's active suspension during the braking procedure is required, so as, reduction of the braking time and distance for all road conditions can be attained in order to improve the safety of the vehicle.

Thus, the motivation of this paper is to develop a control method for the vehicle's active suspension system, that can enhance the braking performance by considerably reducing the braking time and distance, compared to other passive, semi-active and active suspension control methods. The proposed method can be applicable to any vehicle and although it is mainly focused on the emergency braking performance, it considers the passengers' comfort and the energy consumption by the active suspensions.

The aim and the contribution of the paper are summarized as follows:

- The suggested emergency braking control method can reduce the braking time and distance by providing a correct balance in the longitudinal load transfer between the front and rear axles.
- The above is attained by online determining the optimal vehicle's frame pitch angle utilizing the fuzzy-logic technique that acts as a reference signal to a commonly used linear quadratic controller that regulates the operation of the active suspensions.
- Unlike similar published methods, the presented integrated control system considers the braking response of both the front and rear wheels, as well as the dynamic performance of the vehicle.
- The suggested control algorithm is activated only in emergency conditions which are detected by the travel of the braking pedal, pushed by the driver, to avoid unnecessary continual operation and therefore, unnecessary energy consumption.
- The effectiveness and the feasibility of the proposed braking control method is verified through simulation analysis utilizing the Matlab/Simulink software and the operating improvements are validated with selective simulation results in comparison with passive, semi-active and active suspension systems used in the technical literature, for several road conditions.

II. VEHICLE SUSPENSION SYSTEM MODEL

Since the longitudinal response of the vehicle during braking is studied, the half car trailing arm model is employed. By this model, both the vertical vibration and the pitch movement of the vehicle body, as well as the vertical motions of the front and rear wheels during the braking can be effectively considered [36].

Figs. 1(a) and (b) illustrate the half car model when the vehicle is traveling at a certain constant speed and after the deployment of the active suspension system during a braking, respectively. For the sake of generality, the pitch center (PC) is considered different from the vehicle's center-of-gravity (CoG_s), as this occurs for most of the vehicles.

The longitudinal dynamics of the vehicle are expressed by [37]

$$m_{TOT}\ddot{x} = F^f_{w\_x} + F^r_{w\_x} - F^W_x \tag{1}$$

where, m_{TOT} is the total mass of the half vehicle, x and $\ddot{x}$ are the longitudinal displacement and acceleration of the vehicle

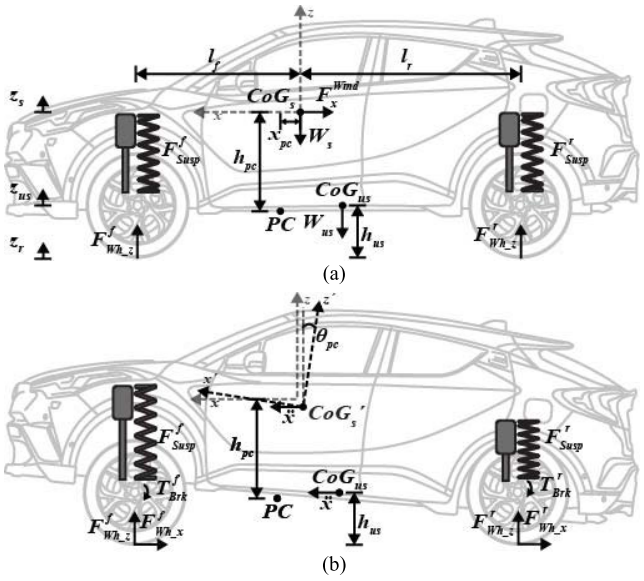

FIGURE 1. Half vehicle suspension model: (a) when it travels at a constant speed and (b) during a braking at the deployment of the active suspension system.

respectively, $F^f_{w\_x}$ and $F^r_{w\_x}$ are the longitudinal forces of the front and rear tires respectively, and F^W_x is the aerodynamic resistance force.

The vertical dynamic of the sprung mass is modeled by

$$m_s\ddot{z}_s = F^f_{Susp} + F^r_{Susp} - m_s g \tag{2}$$

where, m_s is the sprung mass, z_s and $\ddot{z}_s$ are the vertical displacement and acceleration of the chassis, respectively, g is the gravity's acceleration ($g \simeq 9.81\text{m/s}^2$), and F^f_{Susp} and F^r_{Susp} are the front and the rear suspension forces respectively, that are determined by

$$F^i_{Susp} = F^i_{Spr} + F^i_{s\_D} + F^i_{Act} \tag{3}$$

where i denotes the front (f) and the rear (r) suspension, F^i_{Spr} is the spring force, $F^i_{s\_D}$ is the damping force, and F^i_{Act} is the force generated by the actuator of the i-th suspension.

The spring force can be calculated by

$$F^i_{Spr} = K^i_{Spr}(L^i_0 - z^i) \tag{4}$$

where K^i_{Spr} is the stiffness coefficient, L^i_0 is the free length of the i-th suspension and z^i is the deflection that is given by

$$z^i = z_s - z^i_{us} \pm l^i \sin\theta_{pc} \tag{5}$$

where z^i_{us} is the vertical displacement of the unsprung mass, l^i is the distance of the i -th suspension from the CoG $_s$, and θ_{pc} is the pitch angle of the sprung mass in respect to the PC. In (5) the positive sign refers to the front axle, while the negative to the rear axle. Similarly, the damping force can be calculated by

$$F^i_{s\_D} = -C^i_{s\_D}\dot{z}^i \tag{6}$$

where $C^i_{s\_D}$ is the damping coefficient and $\dot{z}^i$ is the vertical velocity of the spring deflection of (5), of the i-th suspension.

Also, the vertical dynamics of the unsprung mass m^i_{us}, that is attributed to the axle of the *i-th* suspension is described by the following expression

$$m^i_{us}\ddot{z}^i_{us} = F^i_{w\_z} - (F^i_{Susp} + m^i_{us}g) \mp L_{us} \tag{7}$$

where, $\ddot{z}^i_{us}$ is the vertical acceleration of the unsprung mass m^i_{us}, $F^i_{w\_z}$ is the vertical force of the *i-th* wheel, h_{us} is the height of the CoG $_{us}$ of the total unsprung mass of the vehicle (front and rear axles), and L_{us} is the longitudinal weight transfer of the total unsprung mass of the vehicle that is given by

$$L_{us} = \frac{(m^f_{us} + m^r_{us})h_{us}\ddot{x}}{l^f + l^r} \tag{8}$$

In (7), the negative sign for the L_{us} corresponds to the front axle, while the positive to the rear axle. Each wheel is simulated as a parallel connected spring and damper system, and thus, the vertical force of the tire is calculated by the following expression

$$F^i_{w\_z} = F^i_{w\_Spr} + F^i_{w\_D} \tag{9}$$

where, the $F^i_{w\_Spr}$ is the wheel's spring force that is given by

$$F^i_{w\_Spr} = K^i_{w\_Spr}[R^i_g - (z^i_{us} - z^i_{road})] \tag{10}$$

where $K^i_{w\_Spr}$ is the spring coefficient, R^i_g is the unloaded geometric radius, and z^i_{road} is the vertical height of the road's disturbance, of the *i-th* wheel. The damping force of the wheel can be calculated by

$$F^i_{w\_D} = -C^i_{w\_D}(\dot{z}^i_{us} - \dot{z}^i_{road}) \tag{11}$$

where $C^i_{w\_D}$ is the damping coefficient and $\dot{z}^i_{road}$ is the vertical velocity, of the *i-th* wheel.

Regarding the rotational dynamics of the system, the moment equilibrium of the sprung mass in respect to its potential rotation around the PC is described by the following relationship

$$J_s\ddot{\theta}_{pc} = F^f_{Susp}l'^f - F^r_{Susp}l'^r + m_s g x_{pc} - m_s h_{pc}(\ddot{x}\cos\theta_{pc} - g\sin\theta_{pc}) \tag{12}$$

where J_s is the inertia of the sprung mass, $\ddot{\theta}_{pc}$ is the acceleration of the pitch angle (that is the angular acceleration of the sprung mass), and x_{pc} and h_{pc} are the longitudinal and vertical distances between the CoG $_s$ and PC, respectively. The longitudinal distances between the PC and the front and rear axles, respectively, are given by

$$l'^f = l^f - x_{pc} \tag{13}$$

$$l'^r = l^r + x_{pc} \tag{14}$$

Thus, considering (2) and (12), and taking into account the moments about the rear and front axles respectively, the front and rear axles' suspension forces in a quasi-steady state condition are given by

$$F^f_{Susp} = \frac{l^r}{l^f + l^r}m_s g + \Delta F_{Susp} \tag{15}$$

$$F^r_{Susp} = \frac{l^f}{l^f + l^r}m_s g - \Delta F_{Susp} \tag{16}$$

where

$$\Delta F_{Susp} = \frac{m_s h_{pc}(\ddot{x}\cos\theta_{pc} - g\sin\theta_{pc})}{l^f + l^r} \tag{17}$$

is the fluctuation in the two axles suspension forces due to a potential pitch rotation of the sprung mass.

The rotational dynamic response of the *i-th* wheel is given by

$$J^i_w\ddot{\theta}^i_w = -T^i_{Brk} + F^i_{w\_x}R^i_w \tag{18}$$

where J^i_w is the inertia, θ^i_w and $\ddot{\theta}^i_w$ are the angle and the angular acceleration, respectively, T^i_{Brk} is the brake torque imposed by the vehicle's braking system, $F^i_{w\_x}$ is the wheel's longitudinal force and R^i_w is the effective radius, of the *i-th* wheel. The effective radius is defined by $R_w = u_x/\omega_w$, where u_x is the longitudinal velocity and ω_w is the angular velocity of the wheel. When the tire is rolling, each part of the circumferences is flattened as it passes through the contact area. Thus,, the R^i_w of each *i-th* wheel is a number between the unloaded geometric radius R^i_g and the loaded height R^i_h ($R^i_h < R^i_w < R^i_g$), and is approximately equal to [38] and [39]

$$R^i_w \approx R^i_g - \frac{R^i_g - R^i_h}{3} \tag{19}$$

The longitudinal force of the *i-th* wheel in relation to the vertical force can be determined by the commonly used magic formula model of Pacejka [40] that is given by

$$F^i_{w\_x} = D^i_x G^i_x + S^i_{Vx} \tag{20}$$

where

$$G^i_x = \sin\left[C^i_x \arctan\left(B^i_x s^i_x - E^i_x\left[B^i_x s^i_x - \arctan\left(B^i_x s^i_x\right)\right]\right)\right] \tag{21}$$

and s^i_x is the longitudinal slip during braking which is defined by [38]

$$s^i_x = \begin{cases} \dfrac{\dot{\theta}^i_w R^i_g - \dot{x}}{\dot{\theta}^i_w R^i_g}, & \dot{\theta}^i_w R^i_g \geq \dot{x} \quad \text{(driving mode)} \\ \dfrac{\dot{\theta}^i_w R^i_g - \dot{x}}{\dot{x}}, & \dot{x} > \dot{\theta}^i_w R^i_g \quad \text{(braking mode)} \end{cases} \tag{22}$$

where $\dot{x}$ is the longitudinal velocity of the vehicle and $\dot{\theta}^i_w$ is the angular velocity of the *i-th* wheel. The values of the parameters B^i_x, C^i_x, D^i_x, E^i_x and S^i_{Vx} of each *i-th* wheel can be determined experimentally.

III. OVERVIEW OF THE PROPOSED CONTROL METHOD

It is well known that the braking performance of a vehicle is considerably influenced by the friction forces at the four tires and the wind resistance. The friction force of each tire depends on the imposed load by the vehicle's weight, its technical characteristics and operating state, and the road's conditions. The force that is owed to the wind resistance

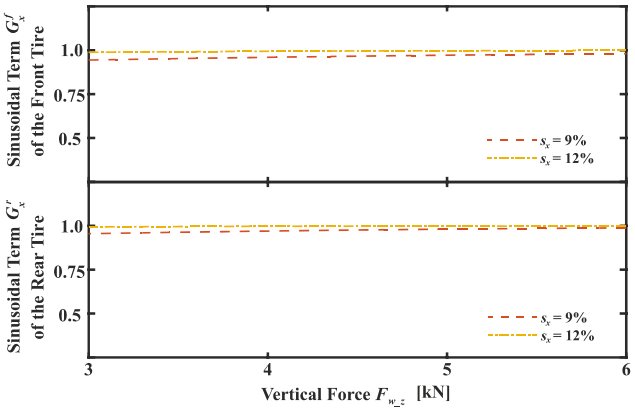

FIGURE 2. Variation of the sinusoidal term Gx of the Pacejka's model versus vertical force, for the front and rear tires, and for several longitudinal slip values.

TABLE 1. Pacejka's model parameters of front and rear tires.

Parameters	Front tire	Rear tire
P_{Cx1}	1.526	1.641
P_{Dx1}	1.091	1.174
P_{Dx2}	-0.153	-0.164
P_{Ex1}	0.432	0.464
P_{Ex2}	0.233	0.250
P_{Ex3}	0.063	0.068
P_{Ex4}	-3.5·10-5	-3.76·10-5
P_{Kx1}	20.74	22.30
P_{Kx2}	0.455	0.489
P_{Kx3}	0.144	0.213
P_{Hx1}	1.14·10-3	1.23·10-3
P_{Hx2}	4·10-4	4.31·10-4
P_{Vx1}	-8.19·10-6	-8.81·10-6
P_{Vx2}	1.73·10-5	1.86·10-5
$F_{w\_z_{nom}}$	4850	4850
$V_{x_{nom}}$	16.6	16.6

depends on the wind's speed and direction, as well as the aerodynamic construction of the vehicle. From the above it follows that for a given vehicle with certain tires', road's and wind's conditions, the braking performance can be enhanced if the vehicle's weight is properly distributed to the four wheels so as their total friction force is increased.

In the Pacejka's magic formula (20), for the *i-th* wheel, the D_x^i determines the amplitude of the sinusoidal variation of the $F_{w\_x}^i$ and assuming pure longitudinal travel (no camber and no slip angle), it can be terms of $F_{w\_z}^i$ by

$$D_x^i = F_{w\_z}^i(P_{Dx1}^i - P_{Dx2}^i) + (F_{w\_z}^i)^2 \frac{P_{Dx2}^i}{F_{w\_z_{nom}}^i} \tag{23}$$

where $F_{w\_z_{nom}}^i$ is the nominal load, and P_{Dx1}^i and p_{Dx2}^i are parameters of the *i-th* tire model. The term S_{Vx}^i shifts the curve of $F_{w\_x}^i(s_x^i)$ not to pass through the origin, due to the rolling resistance and tire irregularities, and it is expressed as

$$S_{Vx}^i = F_{w\_z}^i \frac{P_{Vx2}^i}{F_{w\_z_{nom}}^i} + (P_{Vx1}^i - P_{Vx2}^i) \tag{24}$$

where P_{Vx1}^i and P_{Vx2}^i are parameters of the *i-th* tire model.

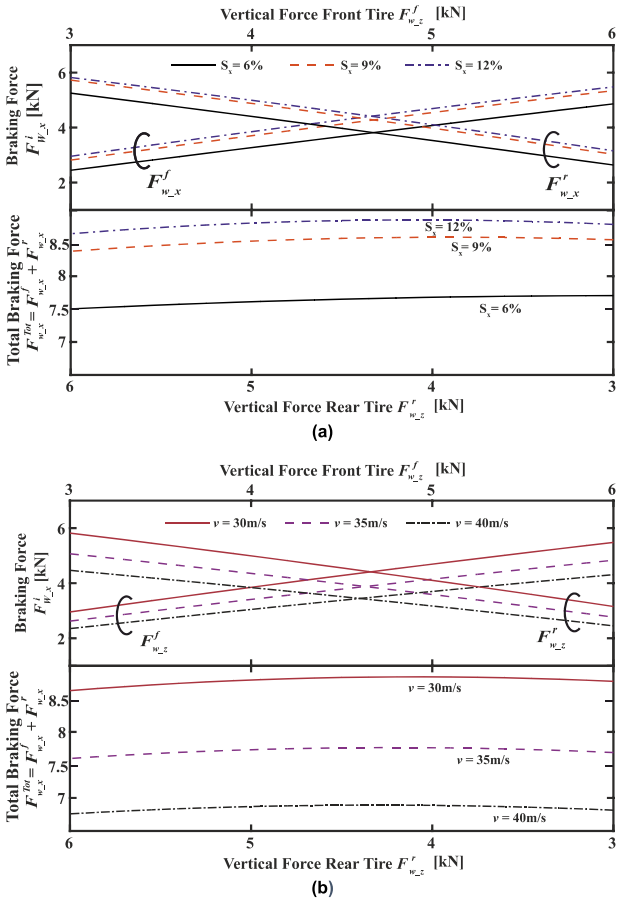

FIGURE 3. Variation of the longitudinal (braking) forces of the front and rear tires, and the total longitudinal (braking) force, versus the front and rear vertical forces, for several wheel slips (s_x) and longitudinal speeds (v), for the Pacejka model's coefficients reported in Table 1.

In the sinusoidal term G_x^i of (21), the stiffness factor B_x^i determines the slope of the $F_{w\_x}^i(s_x^i)$, while the curvature factor E_x^i affects the behavior of the $F_{w\_x}^i(s_x^i)$ at the unstable region (beyond the critical slip s_{x0}^i that corresponds to the maximum value of the longitudinal force). The shape factor C_x^i has a constant value and it describes whether the $F_{w\_x}^i(s_x^i)$ curve is monotonous increasing ($0 < C_x^i < 1$) or includes a local extreme ($C_x^i > 1$).

Although the G_x^i varies with the longitudinal slip s_x^i, its influence by the vertical force $F_{w\_z}^i$ is almost constant in the usual working region of the tire [38]–[40]. The above is validated by the simulation results presented in Fig. 2, that illustrate the variation of G_x^i with respect to the vertical force, for the front and rear tire, and for various longitudinal slip values. The Pacejka's model coefficients of the front and rear tires that have been used for the simulation analysis are reported in Table 1 and are referred to tires of a Class D (Large) vehicle, in consistent with the regulations of [41]. Specifically, two 235/60/R16 tires with unloaded geometric radius R_g of 0.344m are adopted, whose characteristics are obtained by [42]. Note that, the model coefficients of the front tire are different than the rear tire to simulate potential wear unevenness or constructional diversifications.

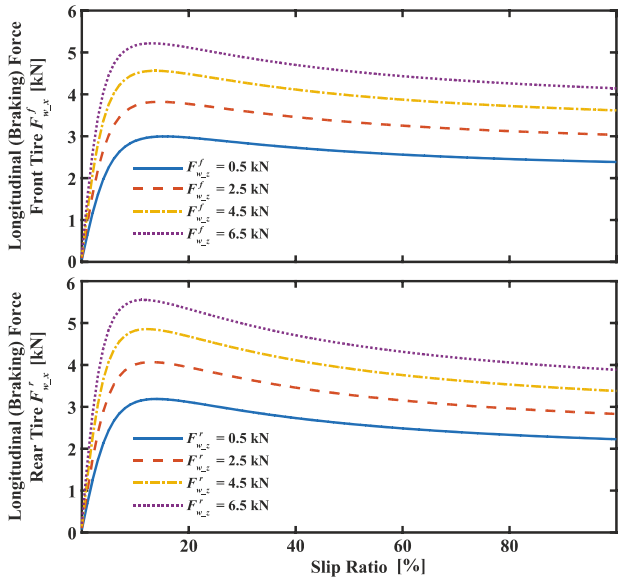

FIGURE 4. Variation of the longitudinal (braking) forces of the front and rear tires (upper and lower diagram, respectively), versus the wheel slip, for several vertical forces.

From (20), (23), (24) and considering the above analysis, it is concluded that, for a given s^i_x longitudinal slip, the variation of $F^i_{w\_x}$ with respect to the vertical force $F^i_{w\_z}$ is almost parabolic and it can be modeled by the following formula

$$F^i_{w\_x} = (F^i_{w\_z})^2 a^i_2 + F^i_{w\_z} a^i_1 + a^i_0 \tag{25}$$

where, for each i-th tire, the a^i_o, a^i_1 and a^i_2 are parameters that depend on the parameters that model the $F^i_{w\_x}$ by (20).

The variation of the longitudinal forces of the front and rear tires ($F^f_{w\_x}$ and $F^r_{w\_x}$, respectively), and the total longitudinal force of the vehicle ($F^{Tot}_{w\_x} = F^f_{w\_x} + F^r_{w\_x}$), versus the front and rear axle vertical forces, for several wheel slips and longitudinal speeds, for the Pacejka model's coefficients reported in Table 1, are illustrated in Fig. 3. As can be observed, the maximum total longitudinal (braking) force of the vehicle is attained for a specific pair of vertical forces of the front and rear tires. In other words, the maximum total braking force can be achieved through the correct distribution of the vehicle's weight to the front and rear wheels that can be accomplished by properly controlling the respective active suspensions.

In the above analysis and also throughout the whole paper, it is considered that the braking system keeps the wheel slip close to the value in which peak deceleration force is generated by alternatively increasing or decreasing the brake torque through the brake valve, as per [35]. The maximum value of the deceleration force at each tire occurs at a specific slip value that, due to the uneven wear, may be different in the two tires. This is validated by the simulation analysis conducted by using the Pacejka's model coefficients of Table 1 and is illustrated in Fig. 4 that presents the variation of the braking forces of the front and rear tires with respect to the longitudinal slip, for several vertical forces.

From the above it is resulted that the stopping time and distance of a vehicle during a braking process can be reduced through a control system, that regulates the active suspension system so as the vehicle's weight is properly allocated between the two axles.

IV. EMERGENCY ACTIVE SUSPENSION CONTROL ALGORITHM

In order to determine the load balance between the front and the rear wheels ($F^f_{w\_z}$ and $F^r_{w\_z}$, respectively), the longitudinal load transfer index (LTI) is introduced, as given by

$$LTI = \frac{F^f_{w\_z} - F^r_{w\_z}}{F^f_{w\_z} + F^r_{w\_z}} \tag{26}$$

Considering (15)-(17) and (7)-(8), it is resulted that the LTI consists of two parts

$$LTI = LTI_U + LTI_C \tag{27}$$

The uncontrollable part LTI_U is given by

$$LTI_U = \frac{\frac{l^r - l^f}{l^f + l^r} m_s + (m^f_{us} - m^r_{us})}{m_s + m^f_{us} + m^r_{us}} + \frac{2\frac{(m^f_{us} + m^r_{us}) h_{us} \ddot{x}}{l^f + l^r}}{(m_s + m^f_{us} + m^r_{us}) g} \tag{28}$$

and it is not affected by the load distribution to the front and rear axles that the suspension system may provide, while the controllable part LTI_C is given by

$$LTI_C = \frac{2 m_s h_{pc} (\ddot{x} \cos\theta_{pc} - g \sin\theta_{pc})}{(l^f + l^r)(m_s + m^f_{us} + m^r_{us}) g} \tag{29}$$

that depends on the pitch angle θ_{pc} and thus, it can be regulated by the active suspension system. Since in most of the vehicles, the pitch angle θ_{pc} that a suspension system can provide does not exceed the 10 °, the LTI_C can be approximated by

$$LTI_C \approx \frac{2 m_s h_{pc} (\ddot{x} - g\theta_{pc})}{(l^f + l^r)(m_s + m^f_{us} + m^r_{us}) g} \tag{30}$$

In addition to attaining maximum total longitudinal force during a braking, the passengers' comfort should be considered, since it affects the sense of safety in the vehicle. Thus, the optimal *LTI* should not only be determined by the proper load balance between the front and the rear wheels, but it depends on the rate of change of the pitch angle. Moreover, the energy consumption by the active suspension operation, during the braking, should be taken into account.

The combined objectives of the proper load balance between the front and the rear wheels, satisfactory comfort and reduced energy consumption during the braking constitute a multi-objective problem that cannot be described by an analytical equation which can serve as an optimal condition. Hence, the fuzzy-logic control technique has been adopted as the most suitable choice to determine in real-time the proper *LTI* that can regulate the vehicle's active suspension system.

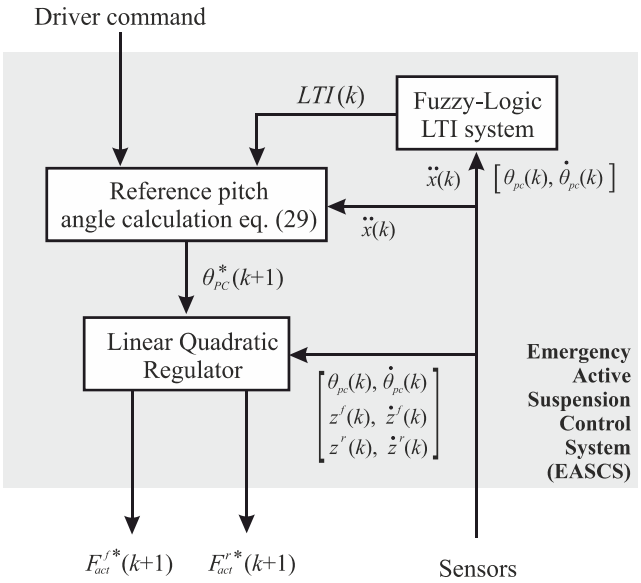

FIGURE 5. Structure overview of the proposed emergency active suspension control (EASC) system.

From (27), (28) and (30) it is concluded that the reference pitch angle can be determined by

$$\theta^*_{pc} = b_2 + b_1\ddot{x} - b_0(LTI) \tag{31}$$

where

$$b_2 = \frac{m_s(l^f - l^r) + (m^f_{us} - m^r_{us})(l^f + l^r)}{2m_s h_{pc}} \tag{32}$$

$$b_1 = \frac{1}{g}\left[\frac{2h_{us}(m^f_{us} + m^r_{us})}{m_s h_{pc}} + 1\right] \tag{33}$$

and

$$b_0 = \frac{(l^f + l^r)(m_s + m^f_{us} + m^r_{us})}{2m_s h_{pc}} \tag{34}$$

Thus, when the emergency braking process is energized, for a given longitudinal deceleration $\ddot{x}$, measured by a sensor, and the optimal *LTI* value provided by utilizing the fuzzy logic technique, the reference pitch angle θ^*_{pc} is determined that the active suspension system should attain.

The structure overview of the proposed emergency active suspension control (EASC) system is illustrated in Fig. 5. As can be seen, it is energized by a command signal that is provided when the travel of the braking pedal pushed by the driver exceeds a specific value. This value characterizes that there is an emergency braking condition and thus, the braking performance should be reinforced. On the other hand, when the travel distance of the braking pedal is below this critical value, it is considered by the system as a smooth braking that can manage it without any additional support. Thereby, energy saving in the active suspensions is accomplished, since it is avoided their unnecessary continual operation for all braking conditions. In the latter case, the active suspension system contributes only to the passengers' comfort.

Inputs to the EASCs are the longitudinal acceleration of the vehicle $\ddot{x}(k)$, the pitch angle $\theta_{pc}(k)$ and its rate of change $\dot{\theta}(k)$, the deflections of the front and rear suspension $z^f(k)$ and $z^r(k)$, respectively, and their respective rates of change $\dot{z}^f(k)$ and $\dot{z}^r(k)$, of the current time step k. The longitudinal acceleration and the pitch angle can be measured by either specific sensors or an Inertial Measurement Unit (IMU) that most of the modern vehicles are usually equipped [43] and [44]. For the measurement of the suspensions' deflections, linear translation sensors can be utilized. Therefore, the proposed emergency active suspension control method is practical to be applied in a vehicle. Then, the reference pitch angle $\theta^*_{pc}(k+1)$ for the next time step $k+1$ is calculated through the condition (31), by utilizing the proper $LTI(k)$, that is determined by a Fuzzy-Logic Reference Generator. Finally, the reference forces of the front and rear active suspension actuators $F^{f*}_{Act}(k+1)$ and $F^{r*}_{Act}(k+1)$, respectively, are calculated by a Linear Quadratic Controller (LQC) as per [46], considering the current values and the rate of change of the pitch angle and the front and rear axle deflection. The goal of the LQC is twofold, the proper control of the vehicle's pitch angle to enhance the braking force at emergency conditions and the passengers' comfort.

It is worth mentioned, that the proposed emergency braking control technique can be applied to active suspensions of either electrohydraulic or pneumatic type, or with electric linear motor actuators. Thus, the output of the LQC is a set of reference forces' signals for the active suspensions of the front and rear axles, that can be utilized by the control drive system depending on their construction type.

A. LTI FUZZY-LOGIC REFERENCE GENERATOR

The LTI Fuzzy-Logic Reference Generator is based on the *Mamdani* type technique [45] and the block diagram is shown in Fig. 6. The goal of the fuzzy-logic algorithm is to provide the proper *LTI* considering the current longitudinal deceleration and pitch angle since they both affect the LTI_C, as can be seen in (29), as well as, the rate of change of the pitch angle, since it affects the passengers' comfort.

The input variable of the longitudinal deceleration $\ddot{x}(k)$ of the vehicle is considered in the normalized form with base value the 1g, which is usually the maximum deceleration that can be attained by a common vehicle. This fuzzy variable is divided into $L = Low$, $M = Medium$ and $H = High$ and the membership functions are illustrated in Fig. 7(a). The fuzzy rule is defined by considering that, if the measured deceleration is in the range of either L or M, the output value of the *LTI* should be selected close to zero, while if it is in the range of H, the *LTI* should increase with high rate. The above fuzzy rule is selected because quick response of the system is required during high deceleration, whereas smooth performance is required when the deceleration decreases.

The pitch angle $\theta_{pc}(k)$ is also considered in normalized form, with base value the 10° which is usually the maximum pitch angle that can be attained by an active suspension

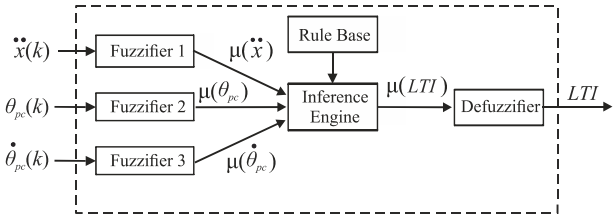

FIGURE 6. Block diagram of the LTI fuzzy-logic reference generator.

system in vehicles. The pitch angle fuzzy variable is divided into *VL=Very Low, L = Low*, *M = Medium*, *H = High* and *VH=Very High* and the membership functions are shown in Fig. 7(b). The concept of the fuzzy rule is based on the equal distribution of the membership functions with respect to the subdivisions of the fuzzy input variable since smooth allocation of the pitch angle with respect to *LTI* is preferred. This fuzzy rule aims to the equal balance between the braking dynamic response and the pitch angle variation, so as unnecessary high oscillations of the active suspension can be avoided and thus, energy saving can be attained.

Finally, the rate of change of the pitch angle $\dot{\theta}_{pc}(k)$ is considered in normalized form as well, by considering the same base value of 10°, as for the pitch angle fuzzy input, which is usually the maximum pitch angle that can be attained by an active suspension system in vehicles. The input fuzzy set is consisted of five membership functions that are illustrated in Fig. 7(c), defined as *NH=Negative High, NL=*Negative *Low*, *Z = Zero*, *PL=Positive Low* and *PH=Positive High*. The opening of the triangle Z membership function is narrower than the other membership functions, since smoothening of the active suspension movement is preferred when the rate of change of the pitch angle has been reduced, in order to increase the passengers' comfort. For the same reason, the slopes of the sides of the NL and PL triangular membership functions towards the Z membership function are lower compared to the other sides. This fuzzy rule aims to provide equal balance between the objectives of improved braking performance and satisfactory passengers' comfort.

The output of the fuzzy system gives the proper *LTI* value and comprises five membership functions illustrated in Fig. 7(d), that are defined as *VL=Very Low, L = Low*, *M = Medium*, *H = High* and *VH = Very High*, respectively. The fuzzy rule of the output membership function is defined on the basis that smooth distribution of the vehicle's weight on the front and rear wheels is required. Thus, the equal distribution of the membership function with respect to the subdivisions of the LTI is set.

B. LINEAR QUADRATIC CONTROLLER (LQC)

As can be seen in Fig. 5, the $\theta^*_{pc}(k+1)$ is provided as input to the LQC that determines the reference forces of the front and rear axles' suspensions, based on the methodology of [5], [46], [47].

Specifically, the output matrix of the reference forces

$$(\boldsymbol{F}^*)^T = \begin{bmatrix} F^{f*}_{Act} & F^{r*}_{Act} \end{bmatrix} \tag{35}$$

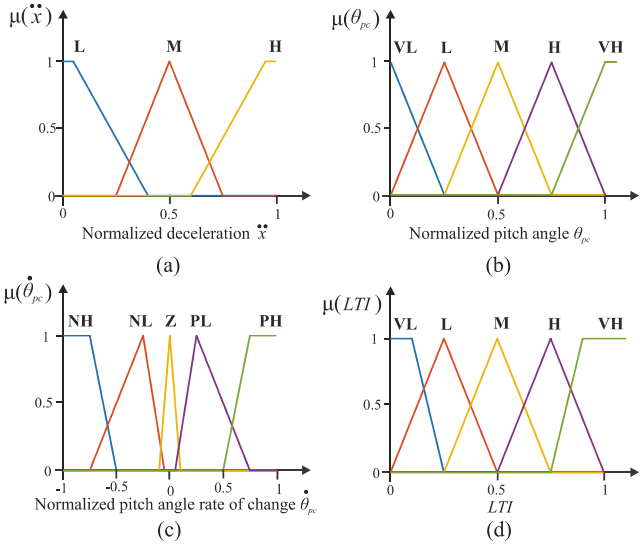

FIGURE 7. Input and output membership functions of the LTI fuzzy-logic reference generator.

is calculated by

$$\boldsymbol{F}^* = -\boldsymbol{G}_F \cdot \boldsymbol{x} \tag{36}$$

where

$$\boldsymbol{x}^T = \begin{bmatrix} z_s & \dot{z}_s & z^f_{us} & \dot{z}^f_{us} & z^r_{us} & \dot{z}^r_{us} & \theta_{pc} & \dot{\theta}_{pc} & e_i \end{bmatrix} \tag{37}$$

e_i is the integral of the error between the reference pitch angle and the actual value, in order to eliminate the steady state error of the controller, and $\boldsymbol{G}_F$ is a gain matrix. The elements of the $\boldsymbol{G}_F$ are determined offline by minimizing the cost function J that is formulated as follows, based on three criteria

$$\min_{\boldsymbol{F}^*} J = J_1 + J_2 + J_3 \tag{38}$$

The criterion J_1 is referred to the referenced vehicles' pitch angle and it is defined as

$$J_1 = \sum_{n=0}^{\infty} q_1[\theta^*_{pc}(n) - \theta_{pc}(n)]^2 \tag{39}$$

The second criterion J_2 corresponds to the reference suspension forces at the front and the rear axles' actuators

$$J_2 = \sum_{n=0}^{\infty} q_2[F^{f*}_{Act}(n) - F^f_{Act}(n)]^2 + q_3[F^{r*}_{Act}(n) - F^r_{Act}(n)]^2 \tag{40}$$

Finally, the third criterion J_3 of the heaving and pitching accelerations is related with the passengers' comfort and it is defined as

$$J_3 = \sum_{n=0}^{\infty} q_4[\ddot{z}^*_s(n) - \ddot{z}_s(n)]^2 + q_5[\ddot{\theta}^*_{pc}(n) - \ddot{\theta}_{pc}(n)]^2 \tag{41}$$

The weight coefficients q_1, q_2, q_3, q_4, and q_5 of (39)-(41) cost function criteria are selected by considering that each

TABLE 2. Class D vehicle's model specifications.

Parameters	Values
Half Vehicle Sprung Weight	800 kg
Front/Rear susp. spring coefficient (K^f_{Spr}, K^r_{Spr})	18/14.5 kN/m
Front/Rear susp. spring free length (L^f_0, L^r_0)	0.5 m
Front/Rear susp. spring damper coefficient ($C^f_{s\_D}, C^r_{s\_D}$)	1.2/1.2 kNs/m
Wheelbase ($l^f + l^r$)	2.5 m
Front Axle Weight Percentage	55%
CoG height	0.67 m
Pitch center height	0.15 m
Pitch center length	0.05 m
Unsprung weight	40 kg
Front/Rear tire spring coefficient ($K^f_{w\ Spr}, K^r_{w\ Spr}$)	210 kN/m
Front/Rear tire geometric radius (R^f_g, R^r_g)	0.344 m
Front/Rear tire damper coefficient ($C^f_{w\_D}, C^r_{w\_D}$)	0.2 kNs/m

criterion has equal effect on the LQC iterative optimization process, as per [48].

Note that the time step k of the LTI fuzzy-logic reference generator may be different than the time step n of the LQC. Both, they are appropriately selected considering that the natural frequency of the sprung mass is in the range of 1-3 Hz, while the natural frequency of the unsprung mass is in the range of 10-12 Hz. Thus, the sampling frequency of the LQC should be at least 10 times greater than the sampling frequency of the LTI fuzzy-logic reference generator. Typical values for the sampling frequency of the LTI fuzzy-logic reference generator and the LQC are 20-25Hz and 200-250Hz, respectively. Also, the close-loop system of Fig. 5 is stable, as it is validated by the stability analysis of [49] which examines the case of close-loop system of an active suspension with an LQC. Note that the reference pitch angle that is determined by the fuzz-logic system and the condition (31) acts as input to the system and thus, it does not affect the stability of the LQC close-loop system.

V. SIMULATION TESTSCASE AND RESULTS

The effectiveness of the proposed EASC system is examined in a half vehicle model by utilizing the Matlab/Simulink software. A Class D vehicle is considered for the simulation analysis and the technical specifications of the model are reported in Table 2. The slip ratio in the tires is optimally controlled by the braking system, so as, maximum braking torque is attained at both front and rear wheels. The simulated actuator is a linear permanent magnet synchronous motor, as per [50]. Its technical specifications are reported in Table 3.

Two scenarios for road condition Class A and Class C according to the ISO 8608:2016 [51] are examined, that correspond to maximum road's irregularities ±5mm and ±25mm, respectively. Thus, both the effectiveness of the EASC system and its impact on the passengers' comfort with respect to the road conditions are studied.

For each of the above road condition scenarios, four cases of suspension systems are comparatively examined.

TABLE 3. Active suspension actuator specifications.

Parameters	Values
Actuator Peak Force	5 kN
Actuator Peak Current	208 A
Actuator Cont. Force	2.25 kN
Actuator Cont. Current	80.5 A

Specifically, the braking performance of the vehicle with the EASC suspension system is compared with a passive suspension called "Passive", a semi-active suspension called "S-Active", and an active suspension technique commonly used in the technical literature, called "Active", which is controlled, so as the pitch angle is kept constantly equal to zero. The model of the S-Active (semi-active) suspension has been obtained by [33].

The starting of the simulations coincides with the initiation of the braking process and when the vehicle runs with a certain longitudinal speed 30m/s (or 108 km/h). The maximum pitch an gle that can be accomplished with any of the examined suspension systems is 10°.

Fig. 8 illustrates the simulation results of the longitudinal and vertical dynamics of the vehicle, for the Class A road scenario. As can be seen, reduction of the stopping distance by 3.9m, 2.63m and 2.5m can be attained with the EASC system compared to the "Passive", "S-Active" and "Active" suspensions, respectively (1st row diagrams), that correspond to reduction of 6.5%, 4.4%, and 4.3%, respectively. This is owed to the faster decrease of the longitudinal velocity (2nd row diagrams) that is resulted by the higher and faster deceleration (3rd row diagrams), which is achieved with the EASC system through the proper control of the vehicle's pitch angle, compared to the other suspension systems. The high oscillations in the longitudinal acceleration (3rd row diagrams) and the vertical acceleration (4th row diagrams) are mainly owed to action of the suspension system against the road irregularities.

Note that, although the stopping distance is reduced with the "Active" compared to the "Passive" and "S-Active" suspensions, further and considerable decrease in the stopping distance is attained with the EASC system, due to the optimal control of the weight distribution of the vehicle between the front and rear axles. The pitch angle is positive with the EASC system indicating that part of the vehicle's weight is transferred from the front axle to the rear one, whereas it is negative in the case of the passive suspension since the front part of the vehicle cannot be lifted and thus, the load distribution follows the natural movement during the braking that is from the rear to the front axle (5th row diagrams). The CoG's vertical displacement is smoother with the EASC and the "Active" suspension that results to higher passengers' comfort compared to the passive suspension (6th row diagram).

The longitudinal and vertical forces, as well as, the actuator force of the front and rear axles, for the Class A road and

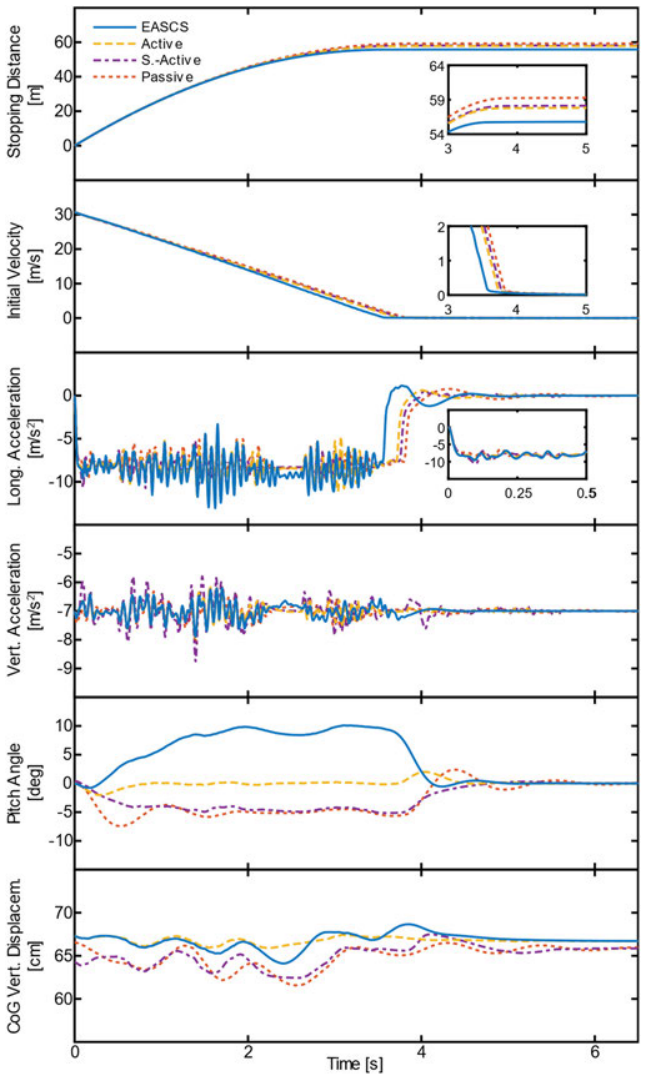

FIGURE 8. Longitudinal and vertical dynamic response of the vehicle, for Class A road with irregularities ±5mm and speed 30m/s, at the initiation of the braking process.

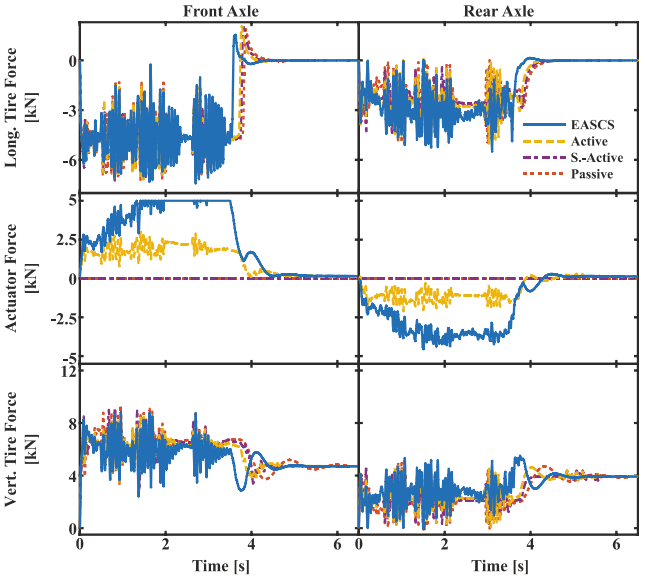

FIGURE 9. Longitudinal and vertical tire forces, as well as, actuator forces of the front and rear axles, for Class A road with irregularities ±5mm and speed 30m/s, at the initiation of the braking process.

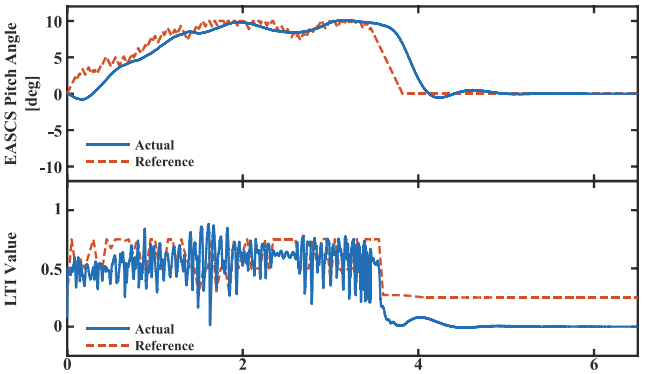

FIGURE 10. EASC system performance, for Class A road with irregularities ±5mm and speed 30m/s, at the initiation of the braking process.

speed 30 m/s at the initiation of the braking, are shown in Fig. 9. As can be seen, due to the proper regulation of the weight between the two axles through the proposed LTI fuzzy-logic reference generator of the EASC system, the longitudinal tire force at the rear axle is increased compared to the other examined suspension systems, while it remains almost unaffected at the front axle (1st row diagrams). This explains the increase of the longitudinal deceleration of the vehicle (3rd row diagrams of Fig. 8) and therefore, the reduction of the stopping time and distance attained with the EASC system, as shown in the 1st row diagrams of Fig. 8. The above is accomplished by the proper control of the front and rear suspensions, as explained by the performance of the respective actuator forces (2nd row diagrams of Fig. 9) and the vertical tire forces (3rd row diagrams of Fig. 9).

The performance of the EASC system is illustrated in Fig. 10. Specifically, the reference and the actual pitch angle are shown in the 1st diagram, while the reference and the actual LTI are illustrated in the 2nd diagram. As can be observed, the actual pitch angle follows the reference signal calculated by the condition (31), but with a small delay that it is owed to the springs response of the suspension system. Similarly, the actual LTI determined by (27) follows the reference signal determined by the LTI fuzzy-logic reference generator of Fig. 6 and the discrepancies are owed to the road irregularities.

Similar results are obtained for the Class C road illustrated in Figs. 11-13, as for the Class A road. In this scenario, the stopping distance is reduced by 3.3m, 1.95m, and 1.8m with the EASC system compared to the "Passive", "S-Active", "Active" suspensions, respectively (1st row diagrams of Fig. 11), that correspond to reduction of 5.3%, 3.2%, and 3%, respectively. The lower reduction in the stopping distance compared to the Class A road is owed to the higher vertical acceleration of the tires caused by the road irregularities that results to reduced tires' braking capabilities (compare the 4th row diagrams of Figs. 8 and 11). The higher oscillations of the CoG's vertical displacement of the Class C road compared

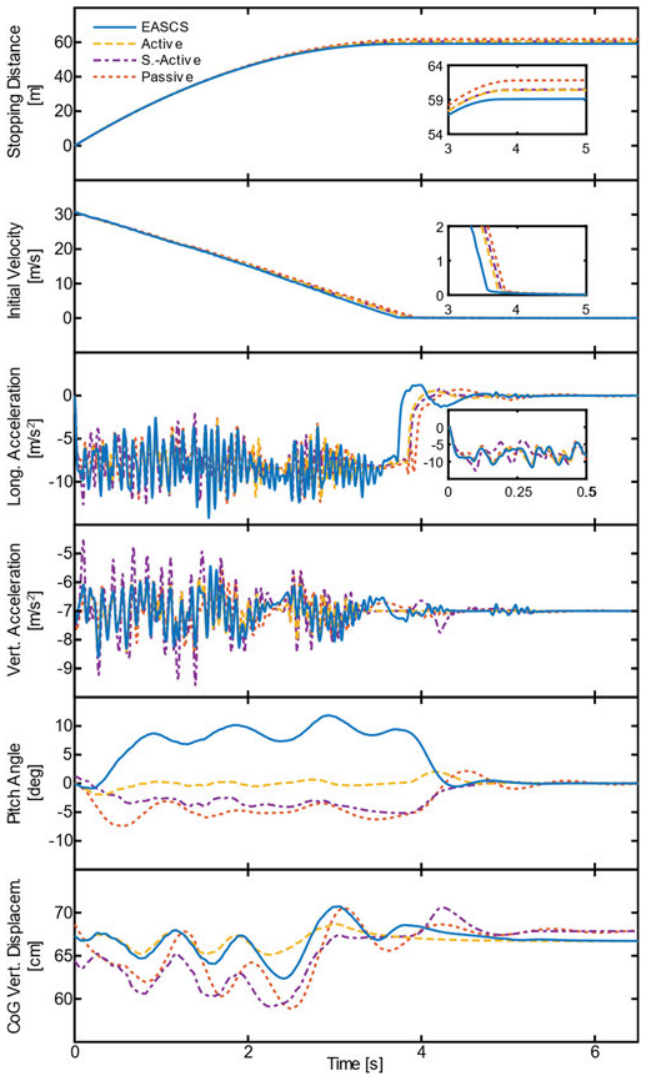

FIGURE 11. Longitudinal and vertical dynamic response of the vehicle, for Class C road with irregularities ±25mm and speed 30m/s, at the initiation of the braking process.

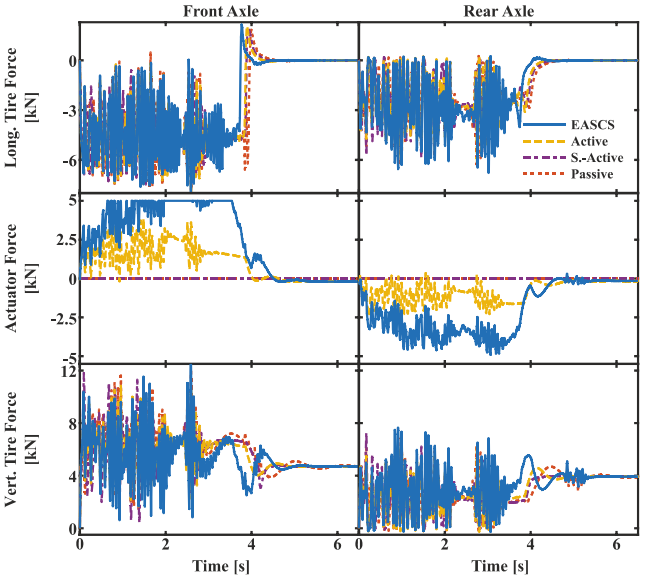

FIGURE 12. Longitudinal and vertical tire forces, as well as, actuator forces of the front and rear axles, for Class C road with irregularities ±25mm and speed 30m/s, at the initiation of the braking process.

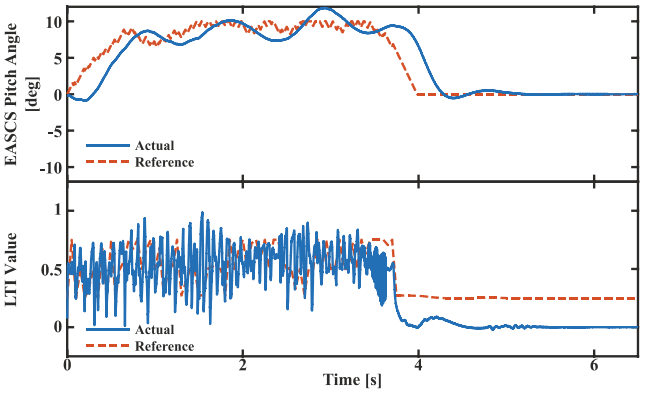

FIGURE 13. EASC system performance, for Class C road with irregularities ±25mm and speed 30 m/s, at the initiation of the braking process.

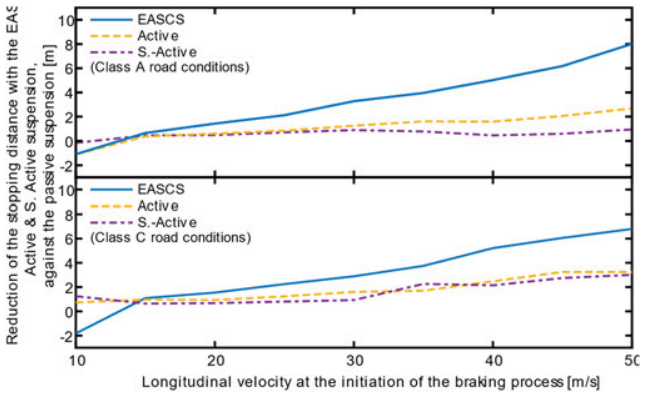

FIGURE 14. EASC system performance, for Class C road with irregularities ±25mm and speed 30 m/s, at the initiation of the braking process.

to Class A are owed to the higher road irregularities (6th row diagrams) that result to slight deterioration of the passengers' comfort. However, these oscillations are considerably lower for the EASC and the "Active" suspensions compared to the "Passive" and "S-Active" suspensions.

Similar conclusions for the longitudinal and vertical tire forces of the Class C road scenario illustrated in Fig. 12 is resulted, as for Class A. However, higher oscillations are observed in the Class C road, due to the higher road irregularities. The same holds for the EASC performance with respect to the pitch angle and the LTI, illustrated in Fig. 13.

Finally, Fig. 14 summarizes the reduction in the stopping distance that can be attained with the EASC, the "Active", and the "S-Active" suspensions against the "Passive" suspension, for Class A and Class C road conditions and for various initial longitudinal speeds. As can be seen, the reduction in the stopping distance is increased as the initial longitudinal speed is increased. Also, higher stopping distance reduction is attained at the Class A road compared to the Class C, due to the lower road irregularities. Although the stopping distance is reduced with the "Active" and "S-Active" suspensions, considerably further reduction can be attained with the EASC system due to the optimal distribution of the vehicle's weight between the front and rear axles. Note that, only in very low

initial speeds (below the 15m/s) and only for the case of Class A road conditions, the passive suspension system slightly outperforms the EASC, ''S-Active'', and the ''Active'' suspension with zero pitch angle. This is owed to the fact that the duration of the braking is very short at the region of very low initial speeds and thus, due to the inertia of the vehicle's sprung mass, the time is not enough to properly distribute the weight between the two axles.

VI. CONCLUSION

In this paper, a control method for the vehicle's active suspension is proposed that can reduce the braking time and distance through a LQC, that properly distribute the sprung mass' weight between the front and rear axles. The LQC is supplemented by a fuzzy-logic reference generator, in order to regulate the actuators' effort. The proposed control method acts in cooperation with the ABS of the vehicle, and it is energized only in an emergency condition which is identified by the travel of the pedal pushed by the driver. The simulation results validate that the stopping distance can be reduced up to 6.5%, 4.4% and 4.3% with the proposed emergency active suspension control method compared to the passive, semi-active and an active suspension technique which is controlled so as the pitch angle is kept constantly equal to zero, respectively, for longitudinal speed 30m/s at the initiation of the braking process. Higher reduction in the stopping distance is attained at smoother roads and for higher initial longitudinal speeds. Finally, the proposed control method outperforms the commonly used in the technical literature active suspension with zero pitch angle, since it increases the total braking force by properly regulating the vehicle's weight to the axles.

REFERENCES

[1] J. C. Dixon, *Suspension Geometry & Computation*. Chichester, U.K.: Wiley, 2009.

[2] S. M. Savaresi, C. Poussot-Vassal, C. Spelta, O. Sename, and L. Dugard, *Semi-Active Suspension Control Design for Vehicles*. London, U.K.: Springer, 2010.

[3] E. Guglielmino, T. Sireteanu, C. W. Stammers, G. Ghita, and M. Giuclea, *Semi-Active Suspension Control*. London, U.K.: Springer, 2008.

[4] H. Liu, H. Gao, and L. Ping, *Handbook of Vehicle Suspension Control Systems*. London, U.K.: Institution of Engineering and Technology, 2014.

[5] P. Brezas and M. C. Smith, ''Linear quadratic optimal and risk-sensitive control for vehicle active suspensions,'' *IEEE Trans. Control Syst. Technol.*, vol. 22, no. 2, pp. 543–556, Mar. 2014.

[6] Y. Zhang and A. Alleyne, ''A practical and effective approach to active suspension control,'' *Vehicle Syst. Dyn.*, vol. 43, no. 5, pp. 305–330, 2005.

[7] S. Lee and W.-J. Kim, ''Active suspension control with direct-drive tubular linear brushless permanent-magnet motor,'' *IEEE Trans. Control Syst. Technol.*, vol. 18, no. 4, pp. 859–870, Jul. 2010.

[8] N. L. V. Truong, V. D. Do, V. T. Nguyen, and P. T. Hai, ''Analytical design of PID controller for enhancing ride comfort of active vehicle suspension system,'' in *Proc. Int. Conf. Syst. Sci. Eng. (ICSSE)*, Jul. 2017, pp. 305–308.

[9] C. Gohrle, A. Schindler, A. Wagner, and O. Sawodny, ''Design and vehicle implementation of preview active suspension controllers,'' *IEEE Trans. Control Syst. Technol.*, vol. 22, no. 3, pp. 1135–1142, May 2014.

[10] C. Gohrle, A. Wagner, A. Schindler, and O. Sawodny, ''Active suspension controller using MPC based on a full-car model with preview information,'' in *Proc. Amer. Control Conf. (ACC)*, Jun. 2012, pp. 497–502.

[11] C. Göhrle, A. Schindler, A. Wagner, and O. Sawodny, ''Road profile estimation and preview control for low-bandwidth active suspension systems,'' *IEEE/ASME Trans. Mechatronics*, vol. 20, no. 5, pp. 2299–2310, Oct. 2015.

[12] D. Wang, D. Zhao, M. Gong, and B. Yang, ''Research on robust model predictive control for electro-hydraulic servo active suspension systems,'' *IEEE Access*, vol. 6, pp. 3231–3240, 2018.

[13] Z. Cao, W. Zhao, X. Hou, and Z. Chen, ''Multi-objective robust control for vehicle active suspension systems via parameterized controller,'' *IEEE Access*, vol. 8, pp. 7455–7465, 2020.

[14] D. Papagiannis, E. Tsioumas, N. Jabbour, M. Koseoglou, and C. Mademlis, ''Fault tolerance in an active suspension system with a linear permanent magnet actuator for automotive applications,'' in *Proc. IEEE Workshop Electr. Mach. Design, Control Diagnosis (WEMDCD)*, Apr. 2019, pp. 203–208.

[15] S. Liu, R. Hao, D. Zhao, and Z. Tian, ''Adaptive dynamic surface control for active suspension with electro-hydraulic actuator parameter uncertainty and external disturbance,'' *IEEE Access*, vol. 8, pp. 156645–156653, 2020.

[16] Y. Zhang, Y. Liu, and L. Liu, ''Adaptive finite-time NN control for 3-DOF active suspension systems with displacement constraints,'' *IEEE Access*, vol. 7, pp. 13577–13588, 2019.

[17] F. Zhao, S. S. Ge, F. Tu, Y. Qin, and M. Dong, ''Adaptive neural network control for active suspension system with actuator saturation,'' *IET Control Theory Appl.*, vol. 10, no. 14, pp. 1696–1705, Sep. 2016.

[18] J. Cao, P. Li, and H. Liu, ''An interval fuzzy controller for vehicle active suspension systems,'' *IEEE Trans. Intell. Transp. Syst.*, vol. 11, no. 4, pp. 885–895, Dec. 2010.

[19] H. Li, H. Liu, H. Gao, and P. Shi, ''Reliable fuzzy control for active suspension systems with actuator delay and fault,'' *IEEE Trans. Fuzzy Syst.*, vol. 20, no. 2, pp. 342–357, Apr. 2012.

[20] D. Liu, H. Chen, R. Jiang, and W. Liu, ''Study of driving performance of semi-active suspension based on hybrid control strategy,'' in *Proc. 2nd WRI Global Congr. Intell. Syst.*, Dec. 2010, pp. 43–46.

[21] R. M. Yerge, P. D. Shendge, V. Paighan, and S. B. Phadke, ''Design and implementation of a two objective active suspension using hybrid skyhook and groundhook strategy,'' in *Proc. 2nd IEEE Int. Conf. Recent Trends Electron., Inf. Commun. Technol. (RTEICT)*, May 2017, pp. 968–972.

[22] M. Čorić, J. Deur, J. Kasać, H. E. Tseng, and D. Hrovat, ''Optimisation of active suspension control inputs for improved vehicle handling performance,'' *Vehicle Syst. Dyn.*, vol. 54, no. 11, pp. 1574–1600, Aug. 2016.

[23] S. Buma, Y. Ookuma, A. Taneda, K. Suzuki, J.-S. Cho, and M. Kobayashi, ''Design and development of electric active stabilizer suspension system,'' *J. Syst. Des. Dyn.*, vol. 4, no. 1, pp. 61–76, 2010.

[24] H. Termous, H. Shraim, R. Talj, C. Francis, and A. Charara, ''Coordinated control strategies for active steering, differential braking and active suspension for vehicle stability, handling and safety improvement,'' *Vehicle Syst. Dyn.*, vol. 57, no. 10, pp. 1494–1529, Oct. 2019.

[25] J. Bengt, *Vehicle Dynamics Compendium*. Gothenburg, Sweden: Chalmers Univ. Technology, 2015.

[26] *Directive on the Approval and Market Surveillance of Motor Vehicles and Their Trailers, and of Systems, Components and Separate Technical Units Intended for Such Vehicles*, document 2018/858/EU, 2018.

[27] *Safety, Comfort and Convenience Systems*, Robert Bosch GmbH, Plochingen, Germany, 2006.

[28] S. M. Saravesi and M. Tanelli, *Active Braking Control Systems Design for Vehicles*. London, U.K.: Springer, 2010.

[29] J. Tjønnås and T. A. Johansen, ''Stabilization of automotive vehicles using active steering and adaptive brake control allocation,'' *IEEE Trans. Control Syst. Technol.*, vol. 18, no. 3, pp. 545–558, May 2010.

[30] S. John, J. O. Pedro, and C. R. Pozna, ''Enhanced slip control performance using nonlinear passive suspension system,'' in *Proc. IEEE/ASME Int. Conf. Adv. Intell. Mechatronics (AIM)*, Jul. 2011, pp. 277–282.

[31] J.-S. Lin and W.-E. Ting, ''Nonlinear control design of anti-lock braking systems with assistance of active suspension,'' *IET Control Theory Appl.*, vol. 1, no. 1, pp. 343–348, Jan. 2007.

[32] T. Niemz and H. Winner, ''Reducing RMS on wheel load in ABS-braking situations by control of semi-active suspension,'' in *Proc. Automot. Syst., Bioeng. Biomed. Technol., Fluids Eng., Maintenance Eng. Non-Destructive Eval., Nanotechnol.*, vol. 2, Jan. 2006, pp. 193–201.

[33] T. Niemz, M. Reul, and H. Winner, ''A new slip controller to reduce braking distance by means of active shock absorbers,'' SAE Tech. Paper 2007-01-3664, 2007.

[34] A. Alleyne, ''Improved vehicle performance using combined suspension and braking forces,'' *Vehicle Syst. Dyn.*, vol. 27, no. 4, pp. 235–265, Apr. 1997.

[35] J. Zhang, W. Sun, and H. Jing, ''Nonlinear robust control of antilock braking systems assisted by active suspensions for automobile,'' *IEEE Trans. Control Syst. Technol.*, vol. 27, no. 3, pp. 1352–1359, May 2019.

[36] F. C. Wang, "Design and synthesis of active and passive vehicle suspensions," Ph.D. dissertation, Dept. Eng., Queen's College, Univ. Cambridge, Cambridge, U.K., 2001. [Online]. Available: https://www.repository.cam.ac.uk/handle/1810/272316
[37] B. Wiegand, "Mass properties and automotive latera accelerators review F," in *Proc. 70th Annu. Conf. Soc. Allied Weight Eng.*, Houston, TX, USA, May 2011, pp. 339–440.
[38] R. N. Jazar, *Vehicle Dynamics*. New York, NY, USA: Springer, 2017.
[39] J. P. Pauwelussen, *Essentials of Vehicle Dynamics*. Oxford, U.K.: Butterworth-Heinemann, 2015.
[40] H. B. Pacejka, *Tyre and Vehicle Dynamics*. Oxford, U.K.: Butterworth-Heinemann, 2006.
[41] *Merger Procedure*, document Regulation (EEC), No 4064/89, 1968.
[42] Mechanical Dynamics Inc. *ADAMS/Car Training Guide*. Accessed: 2001. [Online]. Available: http://www.mscsoftware.com
[43] D. A. Crolla, *Automotive Engineering: Powertrain, Chassis System and Vehicle Body*. Oxford, U.K.: Butterworth-Heinemann, 2009.
[44] Continental. AG, *Inertial Sensor (4DoF)*. Accessed: 2021. [Online]. Available: https://www.continental-automotive.com/en-gl/Trucks-Buses/Vehicle-Chassis-Body/Inertial-Measurement-Sensors
[45] E. H. Mamdani and S. Assilian, "An experiment in linguistic synthesis with a fuzzy logic controller," *Int. J. Man-Mach. Studies*, vol. 7, pp. 1–13, Jan. 1975.
[46] L. Li and F. Y. Wang, *Advanced Motion Control and Sensing for Intelligent Vehicles*. New York, NY, USA: Springer, 2007.
[47] I. Youn, J. Im, and M. Tomizuka, "Level and attitude control of the active suspension system with integral and derivative action," *Vehicle Syst. Dyn.*, vol. 44, no. 9, pp. 659–674, Sep. 2006.
[48] A. G. Thompson, "An active suspension with optimal linear state feedback," *Vehicle Syst. Dyn.*, vol. 5, no. 4, pp. 187–203, Dec. 1976.
[49] G. Koch and T. Kloiber, "Driving state adaptive control of an active vehicle suspension system," *IEEE Trans. Control Syst. Technol.*, vol. 22, no. 1, pp. 44–57, Jan. 2014.
[50] J. Wang and W. Wang, "Testing and experimental characterization of a linear permanent magnet actuator for active vehicle suspension," in *Proc. Int. Conf. Electr. Mach. Syst.*, Aug. 2011, pp. 1–7.
[51] *Mechanical Vibration-Road Surface Profiles-Reporting of Measured Data*, Standard ISO 8608:2016, International Standardization Organization, Geneva, Switzerland, 2016.

DIMITRIOS PAPAGIANNIS was born in Kranea Elassonas, Greece, in December 1990. He received the Diploma degree from the School of Electrical and Computer Engineering, Aristotle University of Thessaloniki, Greece, in 2015, where he is currently pursuing the Ph.D. degree in the area of optimization of vehicles' active suspension systems.

His research interests include the areas of performance improvement of active suspension systems in vehicles, vehicle dynamics, electric motor drives, power electronics, and embedded systems design.

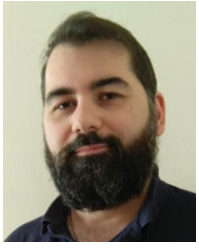

EVANGELOS TSIOUMAS was born in Kompotades Fthiotidas, Greece, in June 1988. He received the Diploma degree from the School of Electrical and Computer Engineering, Aristotle University of Thessaloniki, Thessaloniki, Greece, in 2013, where he is currently pursuing the Ph.D. degree in the area of energy management optimization in microgrids.

His research interests include energy management in power systems, control optimization in microgrids, large-scale electric energy storage systems, and embedded systems design.

MARKOS KOSEOGLOU was born in Thessaloniki, Greece, in July 1992. He received the Diploma degree from the School of Electrical and Computer Engineering, Aristotle University of Thessaloniki, Thessaloniki, Greece, in 2018, where he is currently pursuing the Ph.D. degree in the area of battery management system optimization.

His research interests include energy management in power systems, battery management systems, and embedded systems design.

NIKOLAOS JABBOUR was born in Thessaloniki, Greece, in December 1988. He received the Dipl. Eng. and Ph.D. degrees in electrical and computer engineering from the Aristotle University of Thessaloniki, Greece, in 2012 and 2018, respectively.

Since 2018, he has been with the Electrical Machines Laboratory, School of Electrical and Computer Engineering, Aristotle University of Thessaloniki, as a Postdoctoral Researcher. His research interests include control optimization, electrical machines and drives, power electronics, embedded systems, renewable energy systems, smart grids, and energy management in nearly zero energy buildings.

CHRISTOS MADEMLIS (Senior Member, IEEE) was born in Arnea Chalkidikis, Greece, in February 1964. He received the Diploma degree (Hons.) in electrical engineering and the Ph.D. degree in electrical machines from the Aristotle University of Thessaloniki, Greece, in 1987 and 1997, respectively.

Since 1990, he has been with the Electrical Machines Laboratory, Faculty of Electrical and Computer Engineering, Aristotle University of Thessaloniki, as a Research Associate, from 1990 to 2001; a Lecturer, from 2001 to 2006; an Assistant Professor, from 2007 to 2014; an Associate Professor, from 2014 to 2019; and has been a Professor, since 2019. From 2013 to 2016, he was the Head of the Department of Electrical Energy, and since 2010, he has been the Director of the Electrical Machine Laboratory, Faculty of Engineering, Aristotle University of Thessaloniki. He is the author and coauthor of more than 75 peer-reviewed technical papers. In 2013, he was the Founder and the Faculty Advisor of the Student Formula SAE Racing Team, Aristotle University of Thessaloniki, from 2013 to 2017. In 2017, he was awarded a Fulbright Grant as a Visiting Professor at the APED, Electrical and Computer Engineering Department, University of Connecticut, USA. His research interests include the areas of electrical machines and drives, especially in design and control optimization, renewable energy sources, electric vehicles, energy saving systems, and energy management in nearly zero energy buildings.